

Research Article

An Improved KF-RBF Based Estimation Algorithm for Coverage Control with Unknown Density Function

Lei Zuo , Maode Yan , Yaoren Guo , and Wenrui Ma 

The School of Control and Electronic Engineering, Chang'an University, Xi'an 710064, China

Correspondence should be addressed to Lei Zuo; Lzuo@chd.edu.cn

Received 28 February 2019; Accepted 21 April 2019; Published 3 July 2019

Academic Editor: Xianggui Guo

Copyright © 2019 Lei Zuo et al. This is an open access article distributed under the Creative Commons Attribution License, which permits unrestricted use, distribution, and reproduction in any medium, provided the original work is properly cited.

This paper investigates the coverage control for a group of agents, where the density function over the given region is unknown and time-varying. A cost function, depending on the density function and a certain metric, is provided to evaluate the performance of coverage network. Then, while considering the sampling noise, a novel estimation algorithm is developed to approximate the density function based on the Kalman filter (KF) and the Radial Basis Function (RBF) neural network. Compared with the other estimation algorithms, a novel sampling regulation mechanism is designed to improve the estimation performance and reduce the computational load. On this basis, a coverage control scheme with estimated density function is proposed to drive the agents to the optimal deployment. Moreover, the stability and performance of proposed coverage control system are strictly analyzed. Finally, numerical simulation is provided to illustrate the effectiveness of proposed approaches.

1. Introduction

Recently, the coverage control has received substantially increasing interest, which has emerged in many applications [1–7]. The objective of coverage control is to deploy the agents in a given region, such that the regions with higher interest can get more attentions from the agents. The distribution of this interested information is defined as *density function*. To achieve this goal, a cost function, containing a certain metric and the density function, is provided to evaluate the performance of coverage network. Then, a distributed controller is proposed to minimize this cost function such that the agents can reach the optimal deployment from arbitrary initial positions. It can be seen that the density function plays an important role in coverage control.

Due to the fact that the density function is usually unknown to the agents, the coverage control with unknown density function has been further investigated. Generally, a spatial estimation algorithm is usually developed to approximate the density function. For example, a decentralized adaptive spatial estimation algorithm is developed to approximate the density function for the coverage control in [8]. To verify the effectiveness of this spatial estimation algorithm, an experiment with a group of mobile sensors is presented

in [9]. In our previous work, an efficient coverage algorithm for mobile sensor networks with unknown density function is proposed, where the consensus mechanism is applied to improve the estimation efficiency [10]. More related literature can be found in [11–14].

While considering the sampling noise, the filter algorithms are usually employed to estimate the density function. For instance, the density function over a spatially decoupled scalar field is estimated by using a discrete Kalman filter (KF) based estimation algorithm in [15]. A distributed spatial estimation algorithm based on the Kriging interpolation technique is developed for a group of agents in [16]. The experiment for this KF-based estimation algorithm in coverage control is provided in [17]. To further proceed with the coverage control with unknown density function, a novel estimation algorithm is developed for the coverage network by using the neural network in [18].

When the density function is time-varying, there are also some results to drive the agents to the optimal deployment. In [19], a switching control algorithm with two controllers is proposed, where the first controller is used to compensate for the variation of density function and the second one is to drive the agents to their optimal positions. The coverage control with time-varying density function is also

investigated in [20], in which the density function over this field is continuously growing and cannot be measured by the onboard sensors. Moreover, for the coverage control with unknown and time-varying density function, the Bayesian prediction techniques are employed to estimate the density function in [21].

Although the coverage control with unknown density function has been well studied, there are still many problems in practice. For instance, in [8–10], the density function is estimated based on the noise-free measurements, which limits their applications. For the coverage control with noisy measurements ([15–17]), the state transition matrices in these KF-based estimation algorithms are usually assumed to be known *a priori*. Moreover, in [18, 21], the computational load of the estimation algorithms is heavy. In addition, for most existing coverage control with time-varying density function, the agents are assumed to know the density function *a priori* ([19, 20]). Hence, it is necessary to further investigate the coverage control with both time-varying and unknown density function.

Motivated by this fact, a novel estimation algorithm for density function is developed based on the Kalman filter (KF) and Radial Basis Function (RBF) neural networks. The coverage control scheme with this estimated density function is further proposed in this paper. The main contributions are twofold:

- (i) An improved KF-RBF based estimation algorithm is proposed for the unknown and time-varying density function in coverage control. In this estimation algorithm, the RBF neural network is used to estimate the density function and the related Kalman filter is employed to deal with the noisy measurements. Moreover, a sampling regulation mechanism is designed to improve the estimation efficiency and reduce the computational load. Compared with the existing results in [15–17], the proposed KF-RBF based estimation algorithm can deal with the sampling noise and approximate the time-varying density function without any assumption about the state transition matrices. Moreover, since a sampling regulation mechanism is applied into this estimation algorithm, its computational load is less than the spatial estimation algorithms in [18, 21].
- (ii) Based on the estimated density function, a coverage control strategy is proposed to drive the agents to the optimal deployment. Since the density function is time-varying, the proposed coverage network can effectively adjust the deployment of agents, such that the regions with higher interest could always get more attention from the agents. Moreover, the stability and performance of this proposed coverage control system are strictly analyzed.

The remainder of this paper is organized as follows: The preliminaries and problem formulation are presented in Section 2. An improved KF-RBF based estimation algorithm is developed in Section 3, and the related coverage control scheme is proposed in Section 4. In Section 5, numerical

simulations are provided to verify the proposed approaches. Finally, Section 6 concludes this paper.

2. Preliminaries and Problem Formulation

Consider n agents in a given region Q . The density function over this region is denoted as $\phi(q, t) : \mathbb{R}^2 \rightarrow \mathbb{R}^+$, $q \in Q$. Then, we define the following cost function

$$H(P, t) = \sum_{i=1}^n \int_{W_i} f(p_i, q) \phi(q, t) dq \quad (1)$$

where $P = [p_1, \dots, p_n]^T$ is the position vector of all agents; W_i is the assigned region to the i th agent, and $f(p_i, q)$ is the metric describing the coverage cost from p_i to q .

To quantitatively assess the coverage cost, let $f(p_i, q) = \|p_i - q\|^2$. Then, according to Lloyd algorithm, the Voronoi partition is the optimal strategy for a group of agents in a convex region [22]. That is, the Voronoi region is the optimal assigned region to each agent. The detailed definition of Voronoi region is shown as

$$V_i = \{q \in Q \mid \|q - p_i\|^2 \leq \|q - p_j\|^2, \forall i, j \in n, i \neq j\} \quad (2)$$

where $q \in Q$ is an arbitrary point in Q and V_i is the Voronoi region to the i th agent.

Then, the cost function with quantitative assessment $\|p_i - q\|^2$ and Voronoi region V_i is presented as

$$H(P, t) = \sum_{i=1}^n \int_{V_i} \|q - p_i\|^2 \phi(q, t) dq \quad (3)$$

The objective of coverage control is to minimize the cost function $H(P, t)$ in (3). As $H(P, t)$ is a function in terms of p_i and t , we take the partial derivative of $H(P, t)$ along the trajectory of each agent:

$$\frac{\partial H(P, t)}{\partial p_i} = 2M_{V_i}(p_i - C_{V_i}) \quad (4)$$

where

$$\begin{aligned} M_{V_i} &= \int_{V_i} \phi(q, t) dq \\ C_{V_i} &= \frac{\int_{V_i} q\phi(q, t) dq}{\int_{V_i} \phi(q, t) dq}. \end{aligned} \quad (5)$$

Then, the cost function will reach the minimum when $\partial H(P, t)/\partial p_i = 0$. It leads us to

$$p_i^* = C_{V_i} = \frac{\int_{V_i} q\phi(q, t) dq}{\int_{V_i} \phi(q, t) dq} \quad (6)$$

where p_i^* denotes the optimal position of the i th agent.

On this basis, the optimal deployment for a group of agents is that $p_i = C_{V_i}, \forall i = 1, \dots, n$. Note that the density function $\phi(q, t)$ is necessary to obtain C_{V_i} . However, it is

usually time-varying and unknown to the agents. To this end, an improved KF-RBF based estimation algorithm is designed to approximate the density function, and the coverage control with estimated density function will be proposed in this paper.

Remark 1. In general, the density function $\phi(q, t)$ denotes the distribution of interested information in a given region. In practical cases, the density function has a lot of physical meanings. For instance, the density function can denote the occurrence probability of events in the given region. Then, based on the objective of coverage control, we can effectively drive the agents to the optimal deployment, such that the regions with higher probabilities can get more attention from the agents. One can refer to [23, 24] for more details about the coverage control with detailed density function.

3. The Improved KF-RBF Estimation Algorithm

3.1. Spatial Model. Suppose the agents can measure the density function at its location. Then, the measurements of coverage network are shown as follows.

$$Y(P, t) = [y(p_1, t), \dots, y(p_n, t)]^T \in \mathbb{R}^n \quad (7)$$

As the density function $\phi(q, t)$ is time-varying and the measurements are noise corrupted, a KF-RBF based estimation algorithm will be developed to approximate the $\phi(q, t)$. In the RBF framework, let $\Psi(q) = [\psi_1(q), \dots, \psi_m(q)]^T \in \mathbb{R}^m$ be the basis function. Then, there exists an ideal vector $w \in \mathbb{R}^m$ satisfying [25]

$$Y(P, t) = \Psi^T(P) w \quad (8)$$

where w is the ideal coefficient in RBF framework and $\Psi(P)$ is shown by the following.

$$\Psi(P) = \begin{bmatrix} \psi_1(p_1), & \dots, & \psi_1(p_n), \\ \vdots, & \ddots, & \vdots, \\ \psi_m(p_1), & \dots, & \psi_m(p_n), \end{bmatrix} \in \mathbb{R}^{m \times n} \quad (9)$$

Denote $\hat{\phi}(q, t)$ as the estimated density function. The estimation error $\tilde{\phi}(q, t)$ is shown as

$$\begin{aligned} \tilde{\phi}(q, t) &= \hat{\phi}(q, t) - \phi(q, t) = \Psi^T(q) \hat{w} - \Psi^T(q) w \\ &= \Psi^T(q) \tilde{w} \end{aligned} \quad (10)$$

where \tilde{w} is the estimated coefficient in RBF and $\tilde{w} = \hat{w} - w$.

Particularly, the Voronoi centroid with estimated density function is shown as follows.

$$\hat{C}_{V_i} = \frac{\int_{V_i} q \hat{\phi}(q, t) dq}{\int_{V_i} \hat{\phi}(q, t) dq} \quad (11)$$

Regarding the estimated Voronoi centroid \hat{C}_{V_i} , we have the following definition.

Definition 2. Given a group of agents in the mission region, the coverage network is said to be in a *near-optimal deployment* when all the agents satisfy $\lim_{t \rightarrow \infty} p_i = \hat{C}_{V_i}, \forall i = 1, \dots, n$.

3.2. Sampling Regulation Mechanism. Let $\mathcal{Y}_k \triangleq Y(P, t_k)$. Then, the Pearson Correlation Coefficient between \mathcal{Y}_k and \mathcal{Y}_{k-1} is shown as

$$\begin{aligned} e_s &= \frac{\sum_{j=1}^n (\mathcal{Y}_k(j) - \bar{\mathcal{Y}}_k) (\mathcal{Y}_{k-1}(j) - \bar{\mathcal{Y}}_{k-1})}{\sqrt{\left(\sum_{j=1}^n (\mathcal{Y}_k(j) - \bar{\mathcal{Y}}_k)^2\right) \left(\sum_{j=1}^n (\mathcal{Y}_{k-1}(j) - \bar{\mathcal{Y}}_{k-1})^2\right)}} \quad (12) \end{aligned}$$

where e_s is the Pearson Correlation Coefficient; $\mathcal{Y}_k(j)$ and $\bar{\mathcal{Y}}_k$ denote the j th element and the average of \mathcal{Y}_k at time t_k , respectively.

Let $\Delta t_1(k)$ be the sampling period at t_k . The initial value of Δt_1 is \underline{c} and it satisfies $\underline{c} \leq \Delta t_1(k) \leq \bar{c}$. Then, according to (12), $\Delta t_1(k)$ is adjusted by the following rules:

$$\begin{aligned} \Delta t_1(k+1) &= \begin{cases} \min\{\Delta t_1(k) + \delta, \bar{c}\} & \text{if } 0.9 \leq e_s \leq 1 \\ \max\{\Delta t_1(k) - \delta, \underline{c}\} & \text{if } 0.8 \leq e_s < 0.9 \\ \underline{c} & \text{if } 0 \leq e_s < 0.8 \end{cases} \quad (13) \end{aligned}$$

where δ is a single step in coverage.

From (12), we find that $e_s \in [0, 1]$ and the current measurement \mathcal{Y}_k is more similar to its previous ones when e_s is larger. For instance, when $0.9 \leq e_s \leq 1$, we can increase the sampling period by $\Delta t_1(k+1) = \Delta t_1(k) + \delta$ because the current measurements \mathcal{Y}_k are quite similar to the previous ones \mathcal{Y}_{k-1} . When $0.8 \leq e_s < 0.9$, this shows that the current measurements have a certain variation with their previous ones. Hence, it is necessary to reduce the sampling period by a single step δ . The case $0 \leq e_s < 0.8$ means that the measurements have presented great changes. Then, we directly set the sampling period to its minimum \underline{c} to collect more measurements.

Moreover, to improve the estimation efficiency, we also take the cost function into consideration. Based on the agents' current positions and its estimated Voronoi centroids, we have the following cost functions

$$\hat{H}_a(P, t_k) = \sum_{i=1}^n \int_{V_i} \|p_i - q\|^2 \hat{\phi}(q, t_k) dq \quad (14)$$

$$\hat{H}_e(\hat{\mathcal{C}}_V, t_k) = \sum_{i=1}^n \int_{V_i} \|\hat{C}_{V_i} - q\|^2 \hat{\phi}(q, t_k) dq$$

where $\hat{H}_a(P, t_k)$ is the cost function with current positions and $\hat{H}_e(\hat{\mathcal{C}}_V, t_k)$ is the expected cost function with estimated Voronoi centroids; $\hat{\mathcal{C}}_V = [\hat{C}_{V_1}, \dots, \hat{C}_{V_n}]$.

From (14), it is shown that the \widehat{H}_e is the expected cost function for the coverage network at t_k . Then, define the variation between \widehat{H}_a and \widehat{H}_e as follows.

$$e_h = \left\| \frac{\widehat{H}_a - \widehat{H}_e}{\widehat{H}_e} \right\|^2 = \left\| \frac{\widehat{H}_a}{\widehat{H}_e} - 1 \right\|^2 > 0 \quad (15)$$

$$\{\Delta t_2(k+1), \gamma(k+1)\} = \begin{cases} \{\Delta t_1(k+1), \gamma(k) + \alpha\delta\}, & \text{if } 0 \leq e_h < 0.1 \\ \{\Delta t_1(k+1), \gamma(k) + \delta\}, & \text{if } 0.1 \leq e_h < 0.3 \\ \{\max\{\Delta t_1(k+1) - \delta, \underline{c}\}, \gamma(k)\}, & \text{if } 0.3 \leq e_h < 0.5 \\ \{\max\{\Delta t_1(k+1) - \alpha\delta, \underline{c}\}, \max\{\gamma(k) - \delta, 0\}\}, & \text{if } 0.5 \leq e_h < 1 \\ \{\max\{\Delta t_1(k+1) - 2\alpha\delta, \underline{c}\}, \max\{\gamma(k) - \alpha\delta, 0\}\}, & \text{if } 1 \leq e_h < 2 \\ \{\underline{c}, 0\}, & \text{if } 2 \leq e_h \end{cases} \quad (16)$$

where Δt_2 is the improved sampling period from Δt_1 ; γ denotes the smoothness of cost function; and α is a positive constant.

Compared with (13), Δt_2 is provided to adjust the sampling period based on the cost function variation e_h . In conjunction with (15) and (16), we separate e_h into six parts. For instance, when $0 \leq e_h < 0.1$, the current cost function \widehat{H}_a is close enough to the expected cost function \widehat{H}_e . Hence, we do not need to change the sampling period Δt_1 . When $1 \leq e_h < 2$, it means the \widehat{H}_a has a certain gap with its desired value. Then, we should decrease the sampling period to have more measurements. On this basis, we can effectively obtain an improved sampling regulation rule to estimate the density function.

In addition, the smoothness of cost function is also taken into consideration. We use γ to quantitatively assess the smoothness of cost function. When γ is large enough, the cost function will converge to a stable value. It shows that the coverage procedure is stable with its current measurements. In this case, the sampling period can be further increased. On this basis, we have the following auxiliary sampling rules

$$\Delta t_3(k+1) = \Delta t_2(k+1) + \alpha\delta, \quad \text{if } \gamma(k+1) \geq \eta \quad (17)$$

where Δt_3 is the sampling period regarding both e_h and γ ; η is a positive constant.

Note that there are three levels to regulate the sampling period. We usually take Δt_3 as the final one, because it is calculated by fully considering the coverage procedure and can provide the required measurements properly. To formally illustrate the developed sampling regulation mechanism, we provide Algorithm 1.

Remark 3. Note that the measurement $y(p_i, t)$ and the density function $\phi(p_i, t)$ are the same. Essentially, they both denote the true value of the density function at p_i . $y(p_i, t)$ is the sampling measurement from the i th agent at its current position p_i . $\phi(p_i, t)$ is from the estimation algorithm, which

As the \widehat{H}_e is the cost function with the optimal positions, we have that $\widehat{H}_a \geq \widehat{H}_e$. From (15), it is found that the e_h describes the variation between \widehat{H}_a and \widehat{H}_e . The smaller e_h , the closer \widehat{H}_a and \widehat{H}_e . Particularly, when $\widehat{H}_a = \widehat{H}_e$, the coverage network reaches the optimal deployment. In this case, the sampling period can be further extended. Based on these analyses, we develop the following regulation rules

denotes the ideal approximated value of density function at p_i . It can be presented as $\phi(p_i, t) = \psi^T(p_i)w$, in which the w is the ideal coefficient vector and unknown to the agents.

Remark 4. In the proposed sampling regulation mechanism, the bound values of e_s and e_h are determined by practical requirements. In detail, we should firstly find the boundaries of e_s and e_h based on their definitions. Then, we separate the ranges of e_s and e_h into some subregions by the bound values. These bound values are determined by practical requirements. For instance, $\{\Delta t_2(k+1), \gamma(k+1)\} = \{\Delta t_1(k+1), \gamma(k) + \alpha\delta\}$ if $0 \leq e_h < 0.1$. The range $0 \leq e_h < 0.1$ is given based on practical requirements. When the higher precision is required, one can also set this bound value as $0 \leq e_h < 0.05$, which is essentially more fastidious to the measurements.

Remark 5. It is also worth noting that both the efficiency and accuracy of proposed estimation algorithm are affected by the sampling regulation mechanism. Generally, the smaller of the sampling period, the more accurate of the estimation algorithm. However, it would increase the dimension of measurements, which greatly limits the efficiency of the proposed estimation algorithm. Therefore, the trade-off between the estimation accuracy and efficiency should be taken into consideration while designing the sampling regulation mechanism.

Remark 6. Actually, there are three levels in the proposed sampling regulation mechanism. The first level is based on the variation of measurements, denoted by e_s . Based on the proposed rules in (13), the sampling period will be reduced when the current measurements have a certain variation with its previous ones. Otherwise, it will be extended. The second level is based on the differences between the current cost function \widehat{H}_a and the expected cost function \widehat{H}_e . When \widehat{H}_a has a certain gap from \widehat{H}_e , this means that the estimated errors for density function may be too large for the coverage system.

Require: The positions P ; The estimated density function $\hat{\phi}(q)$; The Voronoi partition $V = \{V_1, \dots, V_n\}$; The measurements \mathcal{Y}_k ; The constant η .

Ensure: The sampling period Δt_3 ;

- (1) Initialization: The coverage step δ ; The boundaries of sampling period \bar{c} and \underline{c} ;
- (2) Calculate the sampling variation e_s based on (12);
- (3) Choose Δt_1 from (13);
- (5) Obtain \hat{H}_a and \hat{H}_e based on the agents' current position p_i and its Voronoi centroids \widehat{C}_{V_i} ;
- (5) Calculate e_h based on (15);
- (6) According to the bound value of e_h in (16), choose the second level sampling period Δt_2 ;
- (7) Based on the smoothness metric γ and its critic η , calculate the final level sampling period Δt_3 through (17).

ALGORITHM 1: The sampling regulation mechanism in coverage control.

Then, we need to collect more measurements to improve the estimation accuracy, which is usually realized by reducing the sampling period. In the third level, we take the smoothness of cost function into consideration. We use γ to illustrate the smoothness of cost function, and the cost function will converge to a stable value if γ is large enough. In this case, the coverage procedure is stable and accurate with its current measurements, which indicates that the sampling period can be further increased. Based on the above three levels in sampling regulation mechanism, we can greatly reduce the computational load and improve the efficiency of proposed coverage system.

3.3. Improved KF-RBF Based Estimation Algorithm. Regarding the proposed sampling regulation mechanism, an improved KF-RBF based estimation algorithm for density function is developed in this subsection.

Depending on the RBF framework, we estimate the density function by

$$\hat{\phi}(q, t) = \Psi^T(q) \hat{w} - c^T(q, P) c^{-1}(P, P) (\Psi^T(P) \hat{w} - Y(P, t)) \quad (18)$$

where $c(\cdot, \cdot)$ denotes the spatial and temporal correlation function between any two points in the given region. For instance, $c(q, P)$ shows the correlation between any point q and the sampling positions P . The detailed formulations of $c(q, P)$ and $c(P, P)$ are presented as

$$\begin{aligned} c_i &= \sigma_r \exp \left[-\frac{(q - p_i)^2}{\sigma_s^2} \right] \exp \left[-\frac{(t - t_i)^2}{\sigma_t^2} \right] \\ c_{ij} &= \sigma_r \exp \left[-\frac{(p_i - p_j)^2}{\sigma_s^2} \right] \exp \left[-\frac{(t_i - t_j)^2}{\sigma_t^2} \right] + \delta_{ij} \end{aligned} \quad (19)$$

where c_i is the i th element in $c(q, P)$ and c_{ij} is the ij th element in $c(P, P)$; σ_r is a constant gain parameter; σ_s and σ_t are spatial and temporal sensitivity parameters, respectively. δ_{ij} is the Kronecker Delta function, which equals 1 if $i = j$ and zeros otherwise.

The objective of this estimation algorithm is to update the coefficient \hat{w} such that the estimation errors $\hat{\phi}(q, t)$ would converge to zeros. The updated law is shown as follows

$$\begin{aligned} \dot{\hat{w}} &= -K_p(t_k) \left(\Psi^T(P) \hat{w}_i - Y(P, t_k) \right) + \Psi^{-1}(P) \left(1 \right. \\ &\quad \left. - \frac{\int_{V_i} \|p_i - q\|^2 \psi(q) dq}{\hat{w}_i - \Psi^{-1}(P) Y(P, t_k)} \right) \Delta Y(P, t_k) \\ &\quad - \int_{V_i} \left[\Psi(P) c^{-1}(P, P) c(q, P) (q - \widehat{C}_{V_i}) \right. \\ &\quad \left. + \psi(q) (q - \widehat{C}_{V_i}) \right]^T dq K(\widehat{C}_{V_i} - p_i) \end{aligned} \quad (20)$$

where $\Delta Y(P, t_k) = (Y(P, t_k) - Y(P, t_{k-1})) / (t_k - t_{k-1})$; K is a positive definite matrix; $K_p(t_k)$ is the gain matrix from Kalman filter, shown as follows

$$\begin{aligned} K_p(t_k) &= P_k(t_{k-1}) \Psi^T(P) (\Psi(P) P_k(t_{k-1}) \Psi^T(P) + R)^{-1} \end{aligned} \quad (21)$$

where R is the noise covariance matrix; $P_k(t_{k-1})$ is the covariance matrix for estimation errors shown by the following.

$$P_k(t_k) = P_k(t_{k-1}) - K_p(t_k) \Psi(P) P_k(t_{k-1}) \quad (22)$$

In this way, the density function at any point q can be approximated by (18), (20), and (21). The K_p in (21) is derived from the Kalman filter, which is used to deal with sampling noise. To fully illustrate the improved KF-RBF based estimation algorithm, we provide Algorithm 2.

In Algorithm 2, the parameters σ_r , σ_s , and σ_t are chosen based on the boundary of density function and the given region. To accurately obtain these parameters, one can use the Monte Carlo and Markov Chain (MCMC) to calculate them iteratively [26]. In addition, while applying Algorithm 2, we have to rasterize the given region to obtain the spatial distribution of density function. In this way, we can calculate the density function point by point and finally get the distribution of density function over the given region.

Require: The sampling measurements $Y(P, t)$ and the agent positions P .

Ensure: The estimated density function $\hat{\phi}(q, t)$

- (1) Initialization: The related parameters $\hat{w}_0, \sigma_r, \sigma_s, \sigma_t, R, P_k(t_0)$; The basis function $\psi(q)$ and the estimation errors critic ξ ;
- (2) **while** $Q \neq \emptyset$ **do**
- (3) $q = q^*$ and $\hat{w} = \hat{w}_0$;
- (4) Compute $\Psi(P), c(q, P)$ and $C(P, P)$ in (18);
- (5) Obtain \hat{C}_{V_i} through the previous estimated density function;
- (6) Calculate the estimation errors $\|\Psi^T(P)\hat{w} - Y(P, t)\|$;
- (7) **while** $\|\Psi^T(P)\hat{w} - Y(P, t)\| > \xi$ **do**
- (8) Calculate $K_p(t_k)$ based on (21);
- (9) Update the covariance matrix $P_k(t_k)$;
- (10) Substitute $K_p(t_k)$ into (20) and obtain the coefficient parameters $\hat{w}(t_{k+1})$;
- (11) Obtain the estimated density function $\hat{\phi}(q, t_{k+1})$ through (18);
- (12) **end while**
- (13) Remove q from Q and choose another point q^* for estimation;
- (14) Update the related variables: $k = k + 1$; $\hat{w}_0 = \hat{w}_{t_{k+1}}$;
- (15) **end while**

ALGORITHM 2: The improved KF-RBF based estimation algorithm.

Remark 7. In addition, the adaptive updated law of \hat{w} in (20) consists of three parts. The first term is used to decrease the estimation errors of density function; the second one can eliminate the influence of time-varying density function in proposed coverage control system; and the last one is to compensate for the distance between the estimated centroid \hat{C}_{V_i} and the real centroid C_{V_i} . In conjunction with these terms, the estimation errors of proposed algorithm will converge to zeros while ensuring the system stability.

4. Coverage Control with Estimated Density Function

In this section, the coverage control scheme with estimated density function is developed. The performance and stability of this proposed coverage control system are further analyzed.

Consider the dynamics of agents as follows

$$\dot{p}_i = u_i, \quad i = 1, \dots, n \quad (23)$$

where u_i is the inputs of each agent.

Regarding the estimated density function $\hat{\phi}(q, t)$, the cost function with estimated density function is presented as follows.

$$\hat{H}(P, t) = \sum_{i=1}^n \int_{V_i} \|q - p_i\|^2 \hat{\phi}(q, t) dq \quad (24)$$

Then, a distributed coverage control law is proposed as follows:

$$u_i = K_c \left(\frac{\int_{V_i} \hat{\phi}(q, t) dq}{\int_{V_i} q \hat{\phi}(q, t) dq} - p_i \right) = K_c (\hat{C}_{V_i} - p_i), \quad (25)$$

$$i = 1, \dots, n$$

where $K_c \in \mathbb{R}^{2 \times 2}$ is the positive definite matrix.

To further analyze the stability of proposed coverage system, a formalized theorem is presented as follows.

Theorem 8. Consider a group of agents in a given region Q , which is described by (23). The sampling regulation mechanism of these agents is presented in (13), (16), and (17). The time-varying density function over given region is approximated through (18). Then, by using the proposed coverage control law in (25), the coverage network will converge to the near-optimal deployment from arbitrary initial positions.

Proof. According to (18), the estimation errors are shown as follows.

$$\begin{aligned} \tilde{\phi}(q, t) &= \hat{\phi}(q, t) - \phi(q, t) \\ &= \Psi^T(q) \tilde{w} - c^T(q, P) c^{-1}(P, P) \Psi^T(P) \tilde{w} \end{aligned} \quad (26)$$

Based on the updated law in (20), $\dot{\tilde{w}}_i$ is presented as

$$\begin{aligned} \dot{\tilde{w}}_i &= -K_p(t_k) (\Psi^T(P) \tilde{w}_i - Y(P, t_k)) + \Psi^{-1}(P) \left(1 \right. \\ &\quad \left. - \frac{\int_{V_i} \|p_i - q\|^2 \psi(q) dq}{\hat{w}_i - \Psi^{-1}(P) Y(P, t_k)} \right) \Delta Y(P, t_k) - \int_{V_i} [\Psi(P) \end{aligned} \quad (27)$$

$$\begin{aligned} &\cdot c^{-1}(P, P) c(q, P) (q - \hat{C}_{V_i}) + \psi(q) \\ &\cdot (q - \hat{C}_{V_i})]^T dq K(\hat{C}_{V_i} - p_i) \\ &= -K_p \Psi^T(P) \tilde{w}_i + \left(1 - \frac{\int_{V_i} \|p_i - q\|^2 \psi(q) dq}{\hat{w}_i} \right) \dot{w} \\ &\quad - A \end{aligned} \quad (28)$$

$$= -K_p \Psi^T(P) \tilde{w}_i + \dot{w} - \int_{V_i} \|p_i - q\|^2 \psi(q) dq \frac{\dot{w}}{\hat{w}_i} - A$$

where

$$A = \int_{V_i} [\Psi(P) c^{-1}(P, P) c(q, P) (q - \widehat{C}_{V_i}) + \psi(q) \cdot (q - \widehat{C}_{V_i})]^T dq K (\widehat{C}_{V_i} - p_i). \quad (29)$$

Then, consider the following Lyapunov function candidate.

$$\mathcal{V} = H + \frac{1}{2} \sum_{i=1}^n \widehat{w}_i^T \widehat{w}_i > 0 \quad (30)$$

Taking the derivative of \mathcal{V} gives the following.

$$\dot{\mathcal{V}} = \sum_{i=1}^n \left(\frac{d}{dt} \int_{V_i} \|p_i - q\|^2 \phi(q, t) dq + \widehat{w}_i^T \dot{\widehat{w}}_i \right) \quad (31)$$

Denote $\dot{\mathcal{V}}_i \triangleq (d/dt) \int_{V_i} \|p_i - q\|^2 \phi(q, t) dq + \widehat{w}_i^T \dot{\widehat{w}}_i$ and we have the following.

$$\begin{aligned} \dot{\mathcal{V}}_i &= \frac{d}{dt} \int_{V_i} \|p_i - q\|^2 \phi(q, t) dq + \widehat{w}_i^T \dot{\widehat{w}}_i \\ &= \frac{\partial}{\partial p_i} \int_{V_i} \|p_i - q\|^2 \phi(q, t) dq \dot{p}_i \\ &\quad + \int_{V_i} \|p_i - q\|^2 \dot{\phi}(q, t) dq + \widehat{w}_i^T \dot{\widehat{w}}_i \\ &= [(M_{V_i} p_i - L_{V_i}) \dot{p}_i] + \int_{V_i} \|p_i - q\|^2 \psi(q) dq \dot{w} \\ &\quad + \widehat{w}_i^T \dot{\widehat{w}}_i \end{aligned} \quad (32)$$

Regarding the estimated density function $\widehat{\phi}(q, t)$, L_{V_i} satisfies the following.

$$\begin{aligned} L_{V_i} &= \widehat{L}_{V_i} - \widetilde{L}_{V_i} = \widehat{M}_{V_i} \widehat{C}_{V_i} - \widetilde{M}_{V_i} \widetilde{C}_{V_i} \\ &= M_{V_i} \widehat{C}_{V_i} + \widetilde{M}_{V_i} (\widehat{C}_{V_i} - \widetilde{C}_{V_i}) \end{aligned} \quad (33)$$

Substituting (25) and (33) into (32), we have the following.

$$\begin{aligned} \dot{\mathcal{V}}_i &= [(M_{V_i} p_i - (M_{V_i} \widehat{C}_{V_i} + \widetilde{M}_{V_i} (\widehat{C}_{V_i} - \widetilde{C}_{V_i}))) \\ &\quad \cdot K_c (\widehat{C}_{V_i} - p_i)] + \int_{V_i} \|p_i - q\|^2 \psi(q) dq \dot{w} + \widehat{w}_i^T \dot{\widehat{w}}_i \\ &= [(-M_{V_i} (\widehat{C}_{V_i} - p_i) - \widetilde{M}_{V_i} \widehat{C}_{V_i} + \widetilde{L}_{V_i}) \\ &\quad \cdot K_c (\widehat{C}_{V_i} - p_i)] + \int_{V_i} \|p_i - q\|^2 \psi(q) dq \dot{w} + \widehat{w}_i^T \dot{\widehat{w}}_i \end{aligned} \quad (34)$$

Particularly for the term $\widetilde{M}_{V_i} \widehat{C}_{V_i} + \widetilde{L}_{V_i}$, we have the following.

$$\begin{aligned} &\widetilde{M}_{V_i} \widehat{C}_{V_i} + \widetilde{L}_{V_i} \\ &= \int_{V_i} ((q - \widehat{C}_{V_i}) c^T(q, P) c^{-1}(P, P) \Psi^T(P) \bar{w}_i \\ &\quad + (q - \widehat{C}_{V_i}) \psi(q)^T \bar{w}_i) dq \end{aligned} \quad (35)$$

As $\dot{\widehat{w}}_i = \dot{\widehat{w}}_i - \dot{w}$, $\widehat{w}_i^T \dot{\widehat{w}}_i$ becomes as follows.

$$\begin{aligned} \widehat{w}_i^T \dot{\widehat{w}}_i &= \widehat{w}_i^T \left(-K_p \Psi^T(P) \bar{w}_i + \dot{w} \right. \\ &\quad \left. - \int_{V_i} \|p_i - q\|^2 \psi(q) dq \frac{\dot{w}}{\bar{w}_i} - A - \dot{w} \right) \\ &= \widehat{w}_i^T \left(-K_p \Psi^T(P) \bar{w}_i - \int_{V_i} \|p_i - q\|^2 \psi(q) dq \frac{\dot{w}}{\bar{w}_i} \right. \\ &\quad \left. - A \right) = -\widehat{w}_i^T K_p \Psi^T(P) \bar{w}_i - \int_{V_i} \|p_i - q\|^2 \psi(q) dq \\ &\quad \cdot \dot{w}_i - \widehat{w}_i^T A \end{aligned} \quad (36)$$

Then, in conjunction with (35) and (36), $\dot{\mathcal{V}}$ can be written as follows.

$$\begin{aligned} \dot{\mathcal{V}} &= \sum_{i=1}^n \left[-M_{V_i} (\widehat{C}_{V_i} - p_i)^T K_c (\widehat{C}_{V_i} - p_i) \right. \\ &\quad \left. - \widehat{w}_i^T K_p \bar{\phi}(q, t) \right] \end{aligned} \quad (37)$$

For the term $\widehat{w}_i^T K_p \bar{\phi}(q, t)$ in (37), we have the following.

$$\widehat{w}_i^T K_p \bar{\phi}(q, t) = \widehat{w}_i^T \Psi(P) \Psi^{-1}(P) K_p \Psi^T(P) \bar{w}_i \quad (38)$$

From the Kalman filter, we notice that the K_p is used to measure the influence of sampling noise covariance matrix R and estimation error covariance matrix P_k . Hence, when R and P_k are approaching zeros, K_p satisfies the following.

$$\lim_{R \rightarrow 0} K_p = \lim_{R \rightarrow 0} \frac{P_k \Psi^T(P)}{\Psi(P) P_k \Psi^T(P) + R} = \Psi^{-1}(P) \quad (39)$$

$$\lim_{P_k \rightarrow 0} K_p = \lim_{P_k \rightarrow 0} \frac{P_k \Psi^T(P)}{\Psi(P) P_k \Psi^T(P) + R} = 0$$

As $\Psi^{-1}(P)$ is positive definite, $\Psi^{-1}(P) K_p$ satisfies the following.

$$\Psi^{-1}(P) K_p \in [0, (\Psi^{-1}(P))^2] \quad (40)$$

Then, we have the following.

$$\widehat{w}_i^T \Psi(P) \Psi^{-1}(P) K_p \Psi^T(P) \bar{w}_i \geq 0 \quad (41)$$

On this basis, $\dot{\mathcal{V}}$ satisfies the following.

$$\begin{aligned} \dot{\mathcal{V}} &= \sum_{i=1}^n \left[-M_{V_i} (\widehat{C}_{V_i} - p_i)^T K_c (\widehat{C}_{V_i} - p_i) \right. \\ &\quad \left. - \widehat{w}_i^T K_p \bar{\phi}(q, t) \right] \leq 0 \end{aligned} \quad (42)$$

On this basis, we obtain that $\mathcal{V} > 0$ and $\dot{\mathcal{V}} \leq 0$ in the given region. Based on the Barbalat's lemma, the proposed coverage system with estimated density function is stable and the agents will asymptotically converge to the near-optimal deployment from arbitrary initial positions. Moreover, as the coverage system converges to the set $\mathcal{V} = 0$, the coefficient w_i satisfies $\lim_{t \rightarrow \infty} \widehat{w}_i^T \widehat{w}_i = 0$. That is, the proposed estimation algorithm for density function will effectively converge to the real density function. \square

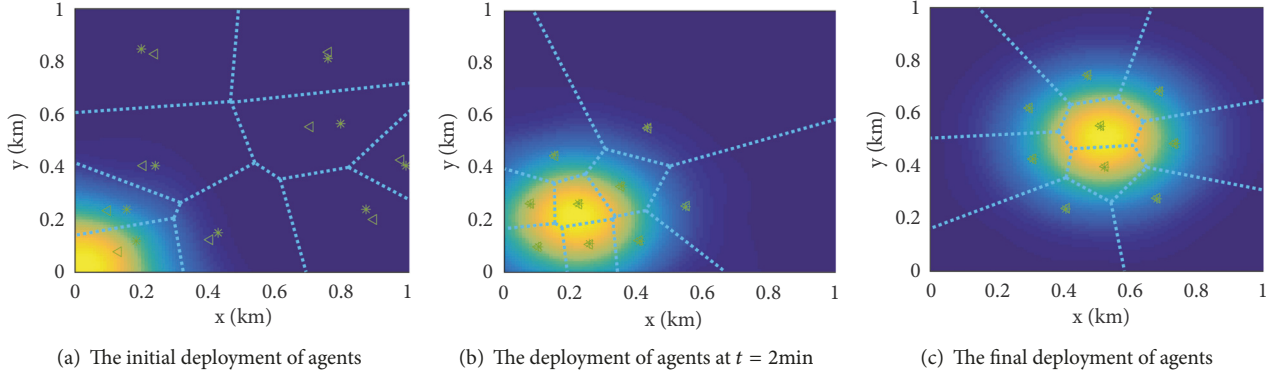


FIGURE 1: The deployment with time-varying density function.

Note that the convergence of estimation algorithm and the stability of proposed coverage control system are both demonstrated in this proof. In (30), the \tilde{w}_i is used to show the convergence of proposed estimation algorithm. As shown in this proof, the \mathcal{V} will converge to the set $\mathcal{V} = 0$ under the proposed control law. From (42), it indicates that $\lim_{t \rightarrow \infty} \tilde{w}_i^T \tilde{w}_i = 0$. That is, the estimation errors of proposed estimated algorithm will converge to zeros. Actually, we can individually prove the convergence of proposed estimation algorithm. However, while applying this estimation algorithm into the coverage system, we must show the convergence of proposed coverage control system with estimated density function.

Based on the proposed coverage control scheme in (25), the agents will converge to the estimated Voronoi centroids $\hat{C}_V, i = 1, \dots, n$. From Definition 2, it is shown that the coverage network can only reach the near-optimal deployment when the density function is unknown to the agents. Actually, while converging the estimated density function to the real one, the near-optimal deployment is almost the same with the real optimal deployment. Hence, it is feasible to put the near-optimal deployment into practice.

5. Simulation

Consider 9 agents in a given region Q ($1\text{km} \times 1\text{km}$). The dynamics of each agent are described by (23), and the density function over this given region is unknown to the agents. Suppose the real density function over Q is described by

$$\begin{aligned} \phi(q, t) &= 1 \\ &+ 1000 \exp\left(-5(2q_x - 2C_x)^2 - 5(2q_y - 2C_y)^2\right) \end{aligned} \quad (43)$$

where $q = [q_x, q_y]^T$ and C_x, C_y are shown as follows.

$$C_x = C_y = \begin{cases} 0.1t, & 0 \leq t < 1.5 \\ 0.15 + 0.01t, & 1.5 \leq t < 7 \\ 0.22 + 0.028t, & 7 \leq t < 10 \\ 0.5, & 10 \leq t \end{cases} \quad (44)$$

From (43), we find that the real density function over the mission region is time-varying and the peak of this density function moves along the diagonal from $(0, 0)$ to $(1, 1)$ with different speeds.

The initial sampling period is $\Delta t_1(0) = 5\text{s}$ and the measurement noise is $\xi \sim \mathcal{N}(0, 1)$. The initial covariance matrices in Kalman filter are $R(0) = I$ and $P_k(0) = I$. In the spatial and temporal correlation function $c(\cdot, \cdot)$, the related parameters are chosen as $\sigma_r = 1, \sigma_s = 2$, and $\sigma_t = 5$. The initial value of coefficient $\tilde{w}(0)$ is random from 1 to 10. On this basis, the numerical results of proposed coverage control system are shown as follows.

Figure 1 illustrates the coverage behaviors of agents with unknown time-varying density function. The star points and triangle points are the agent positions and the Voronoi centroids, respectively. The dashed lines denote the Voronoi partition, and the estimated density function over this given region is presented by the colorful background in Figure 1. The yellow region denotes the peak area of density function, and the detailed values of every kind of colors are presented by the color bar. As shown in Figure 1(a), the initial deployment of agents is randomly located in the given region, and the estimated density function is far away from the real one. Then, in Figure 1(b), the estimation errors for density function converge to zeros and the agents are almost clustered around the peak region of density function. While proceeding the coverage control, all the agents follow the peak of density function and converge to the optimal deployment in Figure 1(c). Regarding Figures 1(a), 1(b), and 1(c), it is shown that the proposed coverage control law can always drive the agents to follow the optimal deployment with time-varying density function. In addition, from background of Figure 1, we can clearly say that the estimated density function strictly follows the moving of real density function, which verifies the effectiveness of proposed estimation algorithm. More detailed analyses are presented in Figures 2, 3, and 4.

The coverage trajectories of all agents are presented in Figure 2, where the circle points are the initial positions, the star points denote the agents' current positions, and the triangle points are the Voronoi centroids. The dashed lines denote the Voronoi partition with the agents' final positions, and the solid lines are the moving trajectories. In Figure 2, we

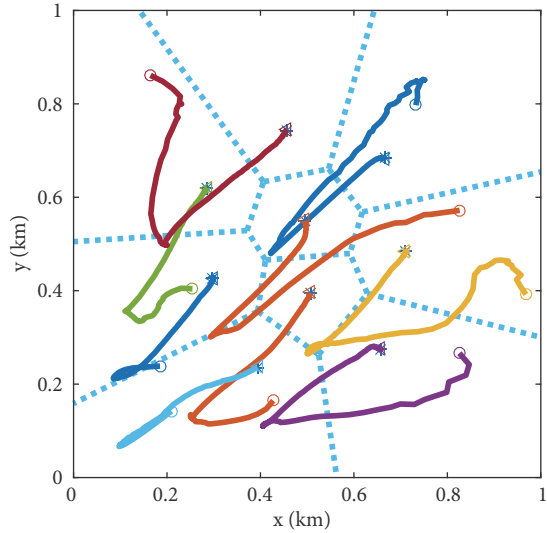


FIGURE 2: The coverage trajectories of agents.

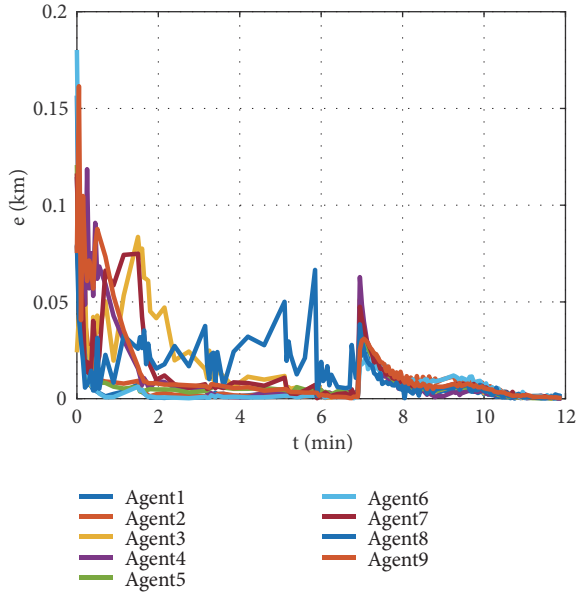
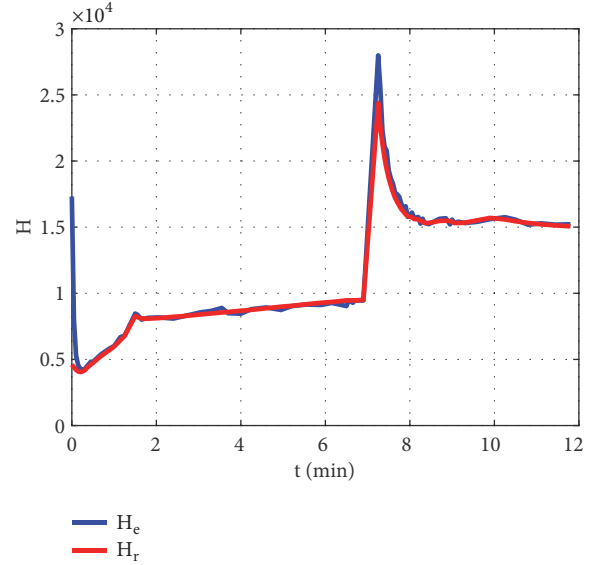


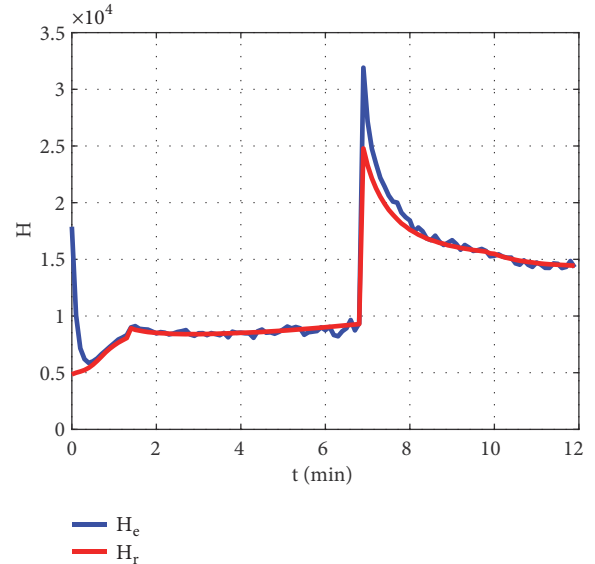
FIGURE 3: The distances from the agents to their centroids.

notice that all the agents move to the lower left corner of the region at the beginning, which is exactly the initial location of the peak of density function. Then, since the peak of density function moves to the center part, the agents are driven to follow the peak such that the regions with higher density can always get more attention from the agents. This result shows that the proposed control strategy can always drive the agents to follow the optimal deployment with time-varying density function.

Figure 3 describes the evolution of the distances from the agents to their centroids. From this figure, we can find that all the agents converge to their centroids, which indicates that the coverage network reaches the optimal deployment. Note that these distances are sometimes increasing during the



(a) The cost function with regulable sampling mechanism



(b) The cost function with fixed sampling mechanism

FIGURE 4: The evolution of the cost function.

coverage procedure. It is because the density function is time-varying and the centroids are closely related to the density function. Hence, the distances between agents and their centroids may be larger when the density function changes its distribution. From another point, this result verifies the advantages of proposed coverage system with time-varying density function.

The evolution of cost function is provided in Figure 4, where Figure 4(a) shows the cost function with proposed sampling regulation mechanism and Figure 4(b) is the cost function with fixed sampling period. In Figure 4, the blue line is the cost function with estimated density function (H_e), and the red line denotes the cost function with real density function (H_r). From Figures 4(a) and 4(b), we can find that

the cost function with estimated density function strictly follows the cost function with real density function, which also verifies the accuracy and efficiency of our proposed coverage scheme and estimation algorithm. Then, comparing Figure 4(a) with Figure 4(b), we find that the convergence rate of cost function with sampling regulation mechanism is obviously larger than the cost function with fixed sampling period. Moreover, the cost function with fixed sampling period shows some chattering during the coverage procedure in Figure 4(b), because the developed sampling mechanism can adjust the sampling period depending on the trend of time-varying density function. For instance, from (43), the peak of real density function changes slowly in 2min to 7min. Then, we extend the sampling period based on the proposed sampling regulation mechanism during this time. However, the fixed sampling mechanism still takes measurement at 5s each time, which also increases the influences of sampling noise. For the evolution of cost function after 7min, Figure 4(a) shows a faster convergence than the cost function in Figure 4(b), because the coverage network with sampling regulation mechanism is more sensitive to the variation of density function. Therefore, the developed sampling regulation mechanism in coverage control reduces the system's computational load and improves the efficiency of proposed coverage system.

6. Conclusion

In this paper, we study the coverage control problems for a group of agents with unknown and time-varying density function. According to the objective of coverage control, a cost function with a certain metric and density function is provided to describe the performance of coverage network. Then, based on the KF and RBF neural network, a novel estimation algorithm is designed to approximate the time-varying density function with noise corrupted measurements. Moreover, a novel sampling regulation mechanism is developed to improve the estimation performance. Regarding the estimated density function, a coverage control scheme is proposed such that the agents can converge to the optimal deployment from arbitrary initial positions. The stability of proposed coverage control system is strictly demonstrated. Finally, numerical simulations are provided to verify the effectiveness of the proposed approaches.

Data Availability

The data used to support the findings of this study are included within the article.

Conflicts of Interest

The authors declare that there are no conflicts of interest regarding the publication of this paper.

Acknowledgments

This work was supported by the National Natural Science Foundation of China (No. 61803040), the Natural

Science Basic Research Plan in Shaanxi Province of China (Nos. 2018JQ6098 and 2019GY-218), and the Fundamental Research Funds for the Central University of China (Nos. 300102328303 and 300102328403).

References

- [1] C. Song, L. Liu, G. Feng, Y. Wang, and Q. Gao, "Persistent awareness coverage control for mobile sensor networks," *Automatica*, vol. 49, no. 6, pp. 1867–1873, 2013.
- [2] J. Cortés, S. Martínez, T. Karataş, and F. Bullo, "Coverage control for mobile sensing networks," *IEEE Transactions on Robotics and Automation*, vol. 20, no. 2, pp. 243–255, 2004.
- [3] T. M. Cheng and A. V. Savkin, "Self-deployment of mobile robotic sensor networks for multilevel barrier coverage," *Robotica*, vol. 30, no. 4, pp. 661–669, 2012.
- [4] F. Bullo, R. Carli, and P. Frasca, "Gossip coverage control for robotic networks: dynamical systems on the space of partitions," *SIAM Journal on Control and Optimization*, vol. 50, no. 1, pp. 419–447, 2012.
- [5] Y. Ru and S. Martínez, "Coverage control in constant flow environments based on a mixed energy–time metric," *Automatica*, vol. 49, no. 9, pp. 2632–2640, 2013.
- [6] H. Xiao, R. Cui, and D. Xu, "A sampling-based bayesian approach for cooperative multiagent online search with resource constraints," *IEEE Transactions on Cybernetics*, vol. 48, no. 6, pp. 1773–1785, 2017.
- [7] Y. Li, R. Cui, Z. Li, and D. Xu, "Neural network approximation based near-optimal motion planning with kinodynamic constraints using RRT," *IEEE Transactions on Industrial Electronics*, vol. 65, no. 11, pp. 8718–8729, 2018.
- [8] M. Schwager, D. Rus, and J.-J. Slotine, "Decentralized, adaptive coverage control for networked robots," *International Journal of Robotics Research*, vol. 28, no. 3, pp. 357–375, 2009.
- [9] M. Schwager, J. McLurkin, and D. Rus, "Distributed coverage control with sensory feedback for networked robots," in *Proceedings of the 2nd International Conference on Robotics Science and Systems, RSS 2006*, pp. 49–56, USA, August 2006.
- [10] L. Zuo, W. Yan, and M. Yan, "Efficient coverage algorithm for mobile sensor network with unknown density function," *IET Control Theory & Applications*, vol. 11, no. 6, pp. 791–798, 2017.
- [11] K. Laventall and J. Cortés, "Coverage control by multi-robot networks with limited-range anisotropic sensory," *International Journal of Control*, vol. 82, no. 6, pp. 1113–1121, 2009.
- [12] L. Zuo, J. Chen, W. Yan, and Y. Shi, "Time-optimal coverage control for multiple unicycles in a drift field," *Information Sciences*, vol. 373, pp. 571–580, 2016.
- [13] M. A. Demetriou and I. I. Hussein, "Estimation of spatially distributed processes using mobile spatially distributed sensor network," *SIAM Journal on Control and Optimization*, vol. 48, no. 1, pp. 266–291, 2009.
- [14] A. Kwok and S. Martinez, "A coverage algorithm for drifters in a river environment," in *Proceedings of the 2010 IEEE American Control Conference (ACC)*, pp. 6436–6441, IEEE, 2010.
- [15] I. I. Hussein, "A Kalman filter-based control strategy for dynamic coverage control," in *Proceedings of the 2007 American Control Conference*, pp. 3271–3276, New York, NY, USA, 2007.
- [16] J. Cortes, "Distributed Kriged Kalman filter for spatial estimation," *IEEE Transactions on Automatic Control*, vol. 54, no. 12, pp. 2816–2827, 2009.

- [17] M. Jadalaha and J. Choi, "Environmental monitoring using autonomous aquatic robots: sampling algorithms and experiments," *IEEE Transactions on Control Systems Technology*, vol. 21, no. 3, pp. 899–905, 2013.
- [18] A. Dirafzoon, S. Emrani, S. M. Salehizadeh, and M. B. Menhaj, "Coverage control in unknown environments using neural networks," *Artificial Intelligence Review*, vol. 38, no. 3, pp. 237–255, 2012.
- [19] X. Liang and Y. Fang, "Time-varying environment coverage control by multi-robot systems," in *Proceedings of the 2015 IEEE International Conference on CYBER Technology in Automation, Control, and Intelligent Systems (CYBER)*, pp. 1940–1945, Shenyang, China, June 2015.
- [20] A. Ghaffarkhah, Y. Yan, and Y. Mostofi, "Dynamic coverage of time-varying environments using a mobile robot - A communication-aware perspective," in *Proceedings of the 2011 IEEE Globecom Workshops*, pp. 1297–1302, IEEE, Houston, Tex, USA, 2011.
- [21] L. Zuo, Y. Shi, and W. Yan, "Dynamic coverage control in a time-varying environment using Bayesian prediction," *IEEE Transactions on Cybernetics*, vol. 49, no. 1, pp. 354–3629, 2019.
- [22] Q. Du, V. Faber, and M. Gunzburger, "Centroidal Voronoi tessellations: applications and algorithms," *SIAM Review*, vol. 41, no. 4, pp. 637–676, 1999.
- [23] J. Clark and R. Fierro, "Mobile robotic sensors for perimeter detection and tracking," *ISA Transactions*[®], vol. 46, no. 1, pp. 3–13, 2007.
- [24] B. A. White, A. Tsourdos, I. Ashokaraj, S. Subchan, and R. Zbikowski, "Contaminant cloud boundary monitoring using network of UAV sensors," *IEEE Sensors Journal*, vol. 8, no. 10, pp. 1681–1692, 2008.
- [25] R. M. Sanner and J. E. Slotine, "Gaussian networks for direct adaptive control," *IEEE Transactions on Neural Networks and Learning Systems*, vol. 3, no. 6, pp. 837–863, 1992.
- [26] C. Andrieu, N. De Freitas, A. Doucet, and M. I. Jordan, "An introduction to MCMC for machine learning," *Machine Learning*, vol. 50, no. 1-2, pp. 5–43, 2003.

